Polym. Bull. (2012) 68:181–196
DOI 10.1007/s00289-011-0548-2

ORIGINAL PAPER

Polyindole–CuO composite polymer electrolyte containing $LiClO_4$ for lithium ion polymer batteries

G. Rajasudha · Larny Mary Jayan ·
D. Durga lakshmi · P. Thangadurai · Nikos Boukos ·
V. Narayanan · A. Stephen

Received: 26 August 2010 / Revised: 9 June 2011 / Accepted: 10 June 2011 /

Abstract This study presents the preparation of a composite polymer electrolyte (CPE), polyindole-based CuO dispersed CPE containing lithium perchlorate by sol–gel method. Morphology and the structural studies were conducted by scanning electron microscopy and X-ray diffraction. The ionic conductivity of CPE was measured for different concentration of the monomer by impedance spectroscopy. CPE containing CuO/indole (2:1 w/w ratio) (CPE3) exhibited enhanced conductivity of 1.9498×10^{-5} S/cm at RT. This CPE showed a linear relationship between the ionic conductivity and the reciprocal of the temperature, indicative of the system decoupled from the segmental motion of the polymer.

Keywords Composite materials · Polymers · Polymer nanocomposite · Ionic conductivity · Polyindole · Polymer electrolyte

Introduction

The polymer–metal oxide nanocomposite have attracted considerable attention worldwide due to their technological applications as electrolytes in all solid-state electrochemical power sources such as rechargeable batteries, fuel cells, supercapacitors etc. All solid-state lithium polymer batteries may be one of the best choices

---

G. Rajasudha · L. M. Jayan · D. Durga lakshmi · A. Stephen (✉)
Department of Nuclear Physics, University of Madras, Guindy Campus, Chennai 600 025, India
e-mail: stephen_arum@yahoo.co.in

P. Thangadurai · N. Boukos
Institute of Materials Science, National Centre of Scientific Research, Aghia paraskevi,
Athens 15310, Greece

V. Narayanan
Department of Inorganic Chemistry, University of Madras, Guindy Campus, Chennai 600 025, India

for the future electrochemical power source characterized by its high energy density, good cyclability, reliability, and safety. The rechargeable Li-ion polymer cells are the key components of the portable, entertainment, computing, and telecommunication equipments used these days. Addition of nanoparticles to the polymer matrix not only lead to the improvement of mechanical strength but also enhances the lithium cation (Li^+) properties such as electrochemical stability and interfacial stability with electrodes [1].

In general, polymer electrolytes may be defined as a membrane having enhanced transport properties comparable with that of the common liquid ionic solution. The conductivity of these polymers can be controlled by changing their redox state by means of chemical or electrochemical reduction or oxidation accompanied by insertion of counter ion [2, 3]. Various methods have been proposed to modify the polymer host matrix with the aim to improve electrolyte utility and in some cases to enhance the mechanical properties of the electrolyte. Addition of nanoparticles of inorganic materials such as Al_2O_3, SiO_2, $LiAlO_2$, and zeolite to polymer electrolytes such as poly ethylene oxide and gel-based systems has been found to improve ionic conductivity to a large extent [4]. By the addition of a small amount of ZnO particles, the ionic conductivity at room temperature of the $(PEO)_{16}$ $LiClO_4$ is enhanced by 40 times, which is attributed to the low crystallinity in the electrolytes resulting from the dispersed ZnO particles [5]. The most promising examples of solid polymer electrolytes are $LiClO_4$-polyethyl-eneoxy, $LiClO_4$-EC (ethylene carbonate), $LiClO_4$-PC (propylene carbonate), $LiClO_4$-DMC (dimethyl carbonate), $LiClO_4$-PVA (polyvinyl alcohol), and $LiClO_4$-lithium polyacrylicate [6].

Polyindole, polypyrrole, polythiophene, and their substituted derivatives have received a great deal of attention because of their good electrical properties, environmental stability, and ease of synthesis. Polyindole has received a significant attention in the past several years. Several reports have been published on polyindole and its derivatives although it’s close structural similarities with polyaniline and polypyrrole. This macromolecular compound is a good candidate for applications in various areas, such as electronics, electrocatalysis, and active materials for batteries, anticorrosion coatings, and pharmacology. The advantages of polyindole consist in a good thermal stability, a high redox activity, a slow degradation rate in comparison with those of polyaniline and polypyrrole and air-stable electrical conductivity close of 0.1 S/cm in the doped state [7]. However, among various aromatic compound-based polymers, polyindole and its derivatives have scarcely been investigated. Polyindole exhibits remarkable electrochemical properties. Polyindole-based aqueous polymer rechargeable battery has a high electromotive force together with a high cycle property and is capable of charging and discharging [8]. Studies on 1D nanomaterials are of great interest due to their unique physical, chemical, optical, and mechanical properties. Among the 1D nanomaterials, primarily we are very much interested in CuO because of its surface catalytic effect and chelating effect, whereas the other conventional metal oxides are having only the surface catalytic effect, which leads to oxidation reaction. The combination behaviors of surface catalytic effect and complex formation effect of CuO urged us to do the present investigation. CuO is a p-type semi conductor with a band gap of 1.2 eV. Various methods are available for the synthesis of such a useful material. CuO may have contributed to dispersion of the filler, thereby enhancing the material's conductivity. In summary, we have synthesized metal oxide with polymer to improve the electrical and thermal conductivity of the polymer composite [9, 10]. In this study, we have prepared polyindole–CuO nanocomposite polymer electrolyte containing $LiClO_4$. Polyindole–CuO nanocomposite was characterized by IR, X-ray diffraction (XRD), scanning electron microscope (SEM), transmission electron microscope (TEM), TGA, and impedance spectroscopy. The $LiClO_4$ was added to the Polyindole–CuO composite to improve the ionic conductivity of the solid polymer electrolyte.

Experimental

Acetonitrile (SD Fine Chemicals) and Ethanol (Changshu Yangyuan Chemical) were distilled and used as solvents. Indole (SD Fine Chemicals) was recrystallized from methanol. Anhydrous ammonium peroxydisulfate (APS) (SRL) was used as the oxidizing agent. Sodium dodecyl sulfate (Rankem) was used as steric stabilizer.

The IR spectrum was recorded using a (Bruker-Tensor 27) Fourier transform IR spectrophotometer. The thermograms were recorded at a heating rate of 10 °C/m using a Perkin-Elmer Thermal Analyzer (Model TGA 7). The morphology was inspected by a (JEOL-JSM-840A) SEM. XRD was performed on a Rich Siefert 3000 diffractometer using Cu $K_{\alpha1}$ radiation ($\lambda = 0.15405$ nm). The lattice parameters were determined and the average crystallite size was estimated using the standard Scherrer formula. Microstructural characterization was performed using the TEM, CM20 (FEI company). Samples for the TEM studies were prepared by dispersing the powder sample in ethanol and sonicated for about 30 min. A drop of the well dispersed particles was smeared on the carbon support membrane of the TEM Cu grid. Ionic conductivities of composite polymer electrolytes (CPEs) were measured by the impedance technique in the frequency range between 5 MHz and 1 Hz on an Impedance Analyzer (Solartron 1260).

Preparation of CPE

Preparation of Polyindole–CuO (PInCuO) nanocomposite

Copper oxide nanoparticle was prepared by chemical method and the details of the synthesis were given elsewhere. The Polyindole–CuO was prepared by chemical method as detailed below. The indole monomer (0.15 g) was dissolved in acetonitrile (50 mL). Copper oxide nanoparticles (1.0 g) were added to the monomer solution under stirring. After 1 h, ammonium peroxydisulfate solution (0.15 g, in acetonitrile 50 mL) was added, and the solution was continuously stirred for 12 h. After 12 h, the supernatant solution was decanted, and the sediment was washed with acetonitrile and water. Then, the solvent was evaporated and dried. Polyindole–copper oxide nanocomposite (PInCuO) was obtained with 80% yield. Similarly, PInCuO nanocomposite with different concentrations of indole (0.15, 0.3, 0.5, 0.75, and 1.0 g of indole with 1.0 g of CuO) were prepared and labeled as S1, S2, S3, S4, and S5. The CuO and PInCuO samples were characterized by IR, XRD, SEM, and TGA.

Preparation of polyindole–CuO CPE with $LiClO_4$ (CPE)

PInCuO nanocomposite (S1, 250 mg) was dispersed in acetonitrile (50 mL) under stirring. $LiClO_4$ (50 mg) was dissolved in acetonitrile. The $LiClO_4$ solution was added to the composite solution under stirring. After 4 h of constant stirring, the solution was evaporated to get polyindole–CuO polymer electrolyte (CPE). Similarly, PInCuO nanocomposites of different concentration (S2, S3, S4, and S5) were treated with $LiClO_4$ to produce CPE containing different monomer concentrations and were labeled as shown in Table 1.

Result and discussions

Structural and microstructural characterization

As the ionic conductivity in a polymer electrolyte is determined by the amorphous nature of the polymer, it is necessary to determine the crystalline and amorphous phases of the polymer electrolyte. Figures 1 and 2 show the XRD patterns of CuO and PInCuO nanocomposite for S1, S2, S3, S4, and S5. The powder XRD patterns of the as-synthesized CuO nanoparticles (Fig. 1) indicate that the particles are of crystalline nature and the peaks are labeled with indexed Bragg reflections of an orthorhombic structure. The XRD pattern of CuO coincides with previous literature and the size of the CuO nano particle is ~ 15 nm as determined by Scherrer formula. In the XRD pattern of PInCuO nanocomposite (Fig. 2), the presence of CuO is observed in addition to the polyindole. Addition of the monomer disrupts the previous ordering, resulting in the reduction of crystallinity of the complex [11]. This observation confirms the complex formation of CuO nanoparticles with polyindole. This can be attributed to increase the amorphous phase of the polymer arising due to destruction of ordered arrangements of polymer chains. With the addition of polyindole, the XRD patterns have exhibited further reduction in the intensity of the Bragg peaks with a diffuse background indicating significant reduction in the crystalline phase [12]. The peaks pertaining to CuO are present in

Table 1 Values of ionic conductivity and activation energy for different composite polymer electrolyte

No.	Label	PInCuO (g)	$LiClO_4$	Ionic conductivity (S/cm) at RT	Activation energy (kJ/mol)
1	CPE1	S1 (250 mg)	50 mg	1.55×10^{-7}	16.36
2	CPE2	S2 (250 mg)	50 mg	1.09×10^{-6}	3.41
3	CPE3	S3 (250 mg)	50 mg	1.95×10^{-5}	3.39
4	CPE4	S4 (250 mg)	50 mg	5.03×10^{-9}	4.50

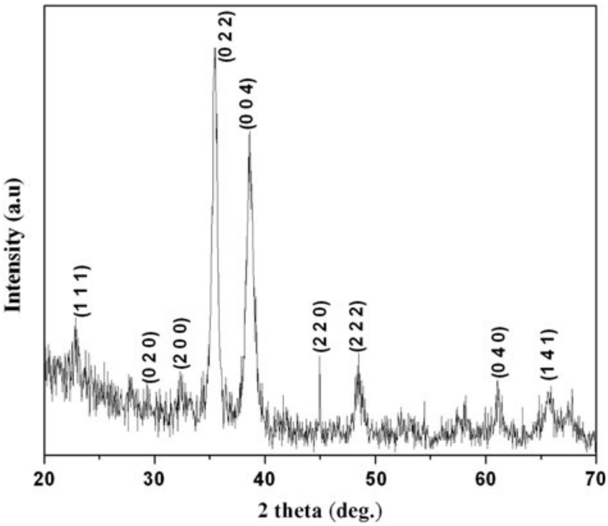

Fig. 1 XRD pattern of CuO nanoparticles

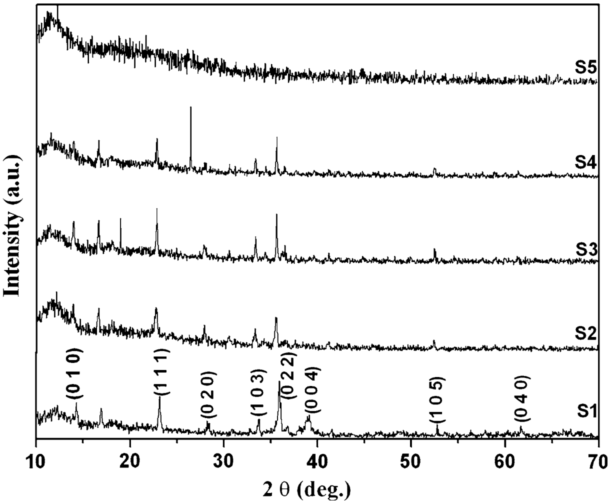

Fig. 2 XRD pattern of polyindole–CuO nanocomposites

the polymer complex with very low intensity due to the interaction between the polyindole and CuO. The XRD pattern of CPE (Fig. 3) shows peaks corresponding to $LiClO_4$ ($2\theta = 22^\circ$). The XRD result reveals the extent of blending of PInCuO nanocomposite with $LiClO_4$ and describes the degree of crystallinity of polymer electrolytes. The same phase of CuO nanoparticles has been retained in their respective nanocomposites with polyindole.

The phase morphology of the electrolytes certainly reflects the possible pathway for ionic movement [13]. SEM image of the CuO nanoparticles (Fig. 4a) and

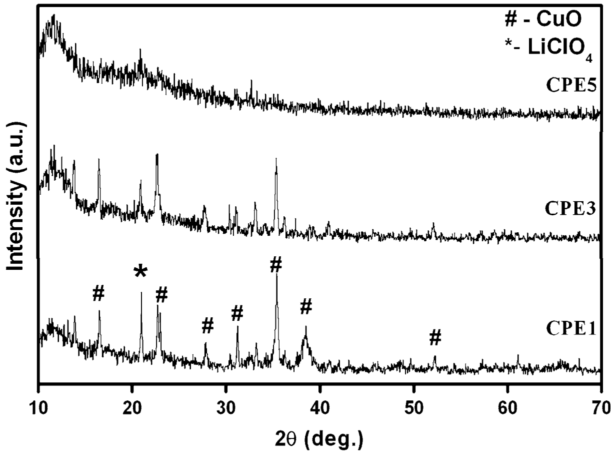

Fig. 3 XRD pattern of Composite polymer electrolyte (CPE1, CPE3, and CPE5)

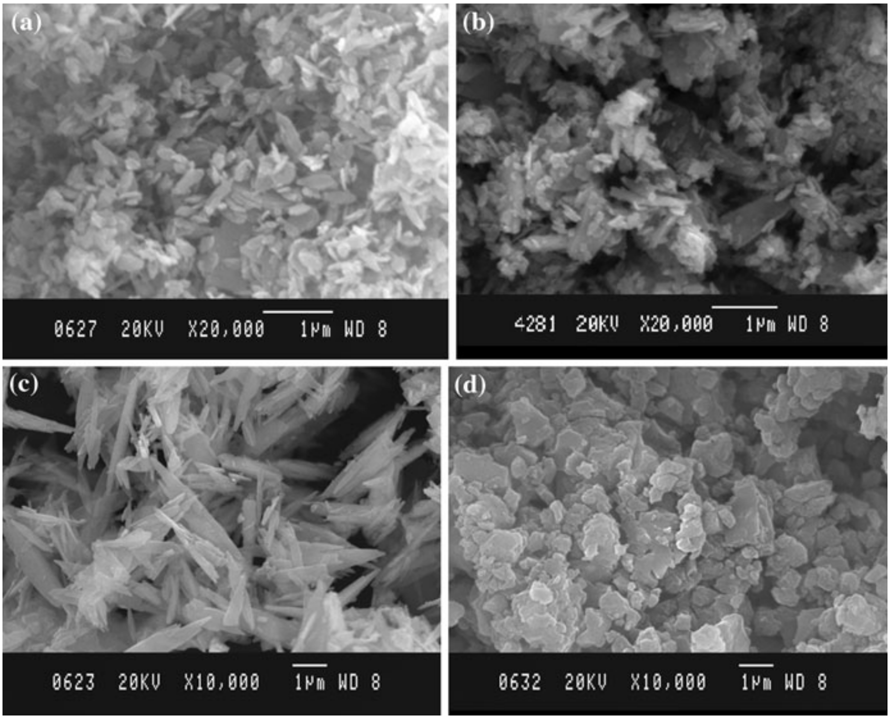

Fig. 4 SEM image of **a** Copper Oxide; **b** PInCuO nanocomposite (S1); **c** PInCuO nanocomposite (S3); **d** PInCuO nanocomposite (S5)

nanocomposite powders for S1, S3, and S5 are shown in Fig. 4b, c, and d, respectively. The needle-shaped CuO nanoparticles are agglomerated (Fig. 4a). The SEM image of S1 nanocomposite obtained with 0.15 g of indole monomer shows

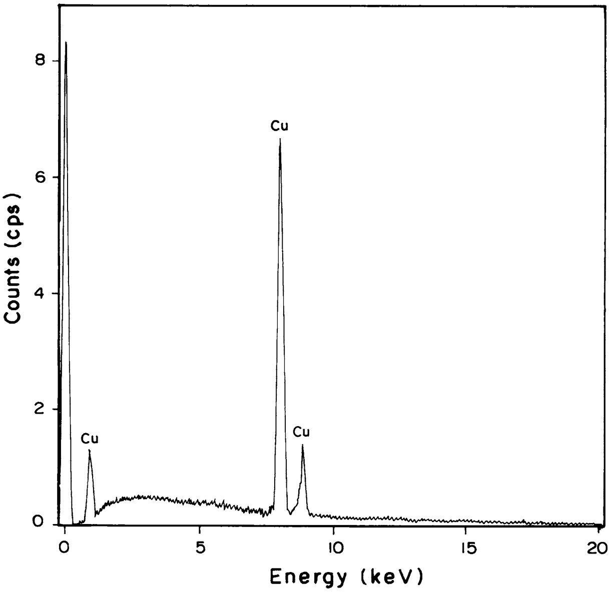

Fig. 5 EDAX spectrum of S1

clusters of needle-shaped particles (Fig. 4b). As the concentration of indole is increased to 0.5 g, the particles become slightly elongated (Fig. 4c). When the concentration of indole is further increased to 1 g, morphology has totally changed and polyindole matrices are observed in Fig. 4d. It is probable that at lower concentrations the oxide is encapsulated by the polymer and with increasing monomer concentration, more and more polymerization gives rise to chain pattern as observed. A further increase in the indole concentration does not result in chain formation but rather a matrix formation. The high Cu ratio in the sample S1 is confirmed by EDAX analysis (Fig. 5). The spectrum shows the peak corresponding to Cu, and this indicates the incorporation of CuO in the polyindole and it confirms the formation of polyindole–CuO composite.

Figure 6a shows the high resolution TEM micrograph of the pure CuO nanoparticles used to make the PInCuO nanocomposite, and its inset shows the Fourier transform of the area marked by a dashed rectangle. The spots shown in the FT image corresponds to the interplanar spacing (*d* spacing) of 2.75 Å that is the (110) plane of CuO. Chemical composition and purity of the CuO particles were studied by electron energy loss spectroscopy (EELS). Figure 6b shows the EELS spectra of CuO particles showing O-K and Cu-$L_{2,3}$ edges, and no other elements were found in it. Background subtraction for the core-loss edges was carried out using the power law model of the form $I = A{\cdot}E^{-r}$, where A and r are fitting parameters.

The TEM microstructure of S1 composite particles in the colloid dispersion with polyindole and CuO particles are shown in Fig. 7a. The particles have aggregated into a rod shape. This should be attributed to the high surface energy of

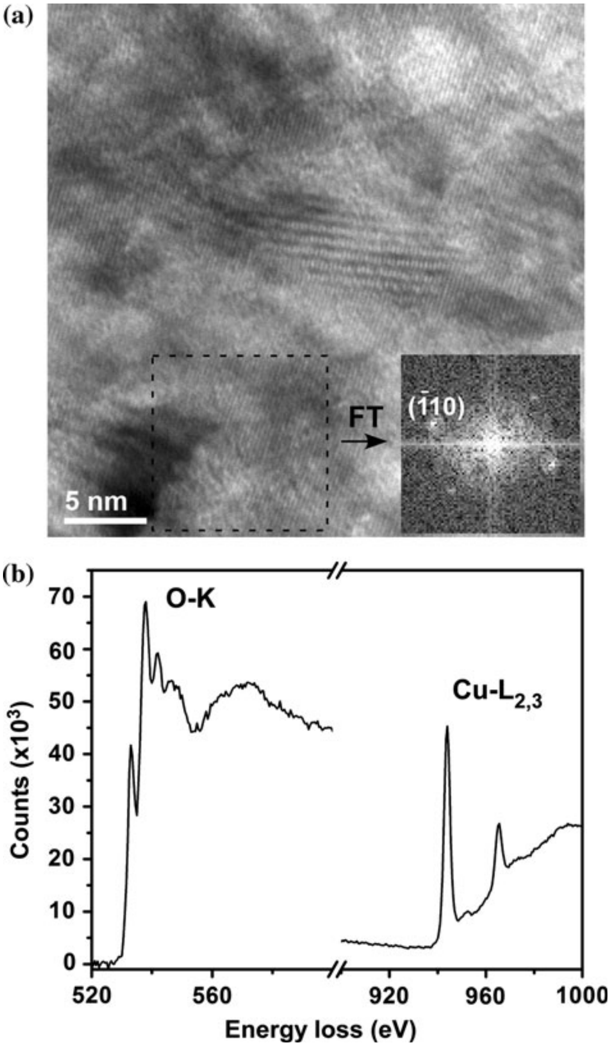

Fig. 6 **a** High resolution TEM micrograph of pure CuO particles used to make the nanocomposite. Inset of **a** is the FT of the region marked by *dashed rectangle*. **b** Electron energy loss spectrum showing the chemical composition of CuO

nanoparticles. It can be seen that most of the composite particles are rod-shaped with length 200–300 nm and with diameter 80 nm. XRD pattern of PInCuO nanocomposite reveals that growth direction of the nanorod is in (022) direction. This kind of growth may be attributed due to the stacking of crystals in this particular direction. The selected-area electron diffraction (SAED) pattern (Fig. 7b) shows a set of diffraction rings due to the random orientation of the nanoparticles, of which the three inner most rings correspond to (020), (022), (004), (222), and (040) planes of the orthorhombic CuO phase. This result is also supported by that obtained from XRD patterns.

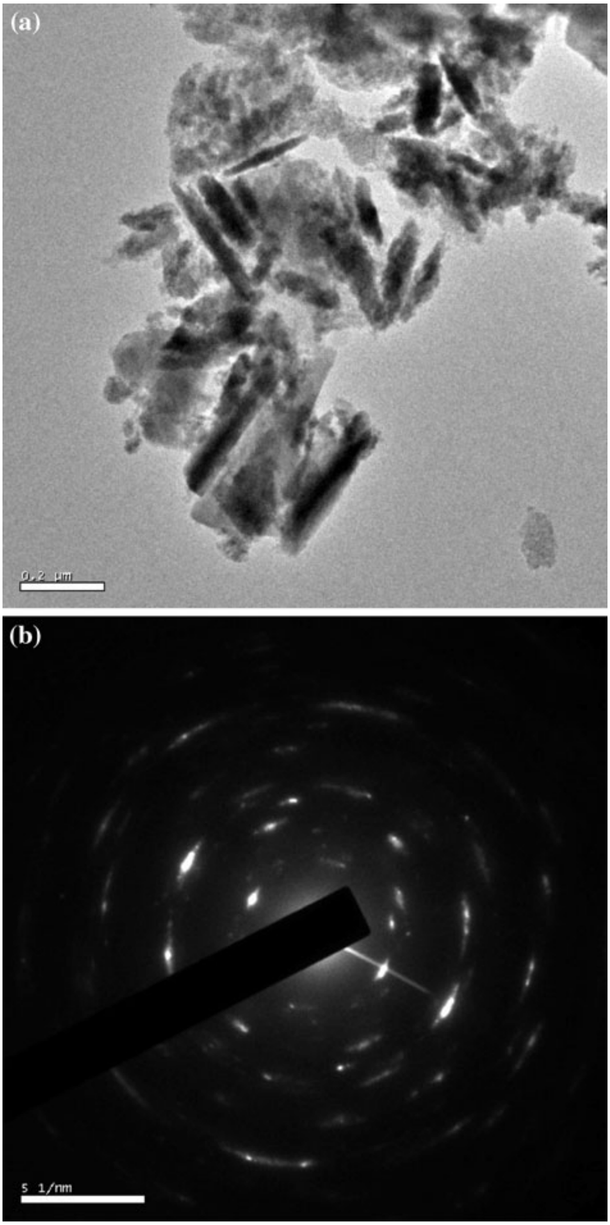

Fig. 7 **a** TEM image of S1 and **b** SAED pattern of S1

Thermal analysis

Thermal characterization of polymeric materials covers many aspects of material science. Thermal studies of polymer electrolytes will provide information with regard to their thermal stability [14]. Weight losses obtained from the TGA graphs

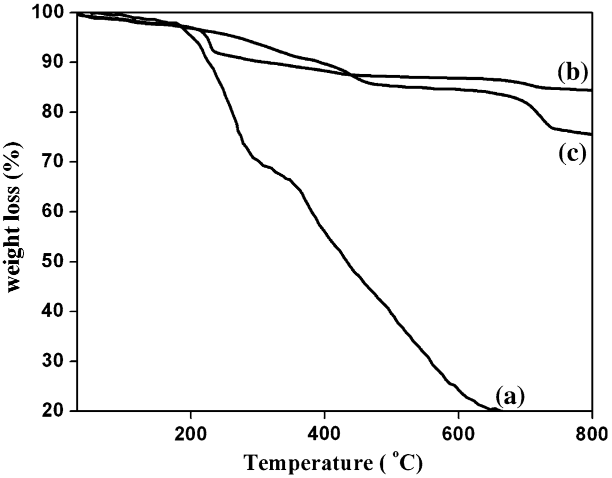

Fig. 8 Thermal analysis (*a*) Polyindole; (*b*) Copper Oxide; and (*c*) PInCuO nanocomposite (S1)

ascertain thermal stability of the polymer electrolyte systems. Figure 8 shows the thermogravimetric analysis (TGA) for polyindole, CuO, and PInCuO system. The weight losses due to evaporation of the physically adsorbed moisture are observed in the curves as shown in Fig. 8a, b, and c at a temperature lower than 200 °C for polyindole and 250 °C for CuO and PInCuO. The decomposition initiates at temperatures higher than 300 °C for polyindole and it is decomposed completely around 630 °C (Fig. 8a). In the case of PInCuO (S1), decomposition starts at 450 °C as shown in Fig. 8c, the resistance to thermal degradation has improved after the nanoparticles were treated with polyindole, indicating a strong interaction between the nanoparticles and polymer matrix [15]. Thermal degradation study by TGA shows an increased thermostability of the nanoparticles containing nanocomposites. Thus, polymer–inorganic nanocomposites prepared through in situ polymerization tend to exhibit enhanced thermal stability compared to the pure polymer. The significant enhancement of thermal stability by incorporating inorganic phase into the polymer matrix is attributed to the strong interfacial interactions between the polymer molecules and inorganic fillers.

Ionic conductivity studies

The ionic conductivity of the CPE was calculated from the impedance spectra. A typical Nyquist plot of the impedance data is shown in Fig. 9. The presence of a semicircle followed by a linear spike at low frequency range at ambient temperatures, as shown in above figure, is similar to what is reported in the literature. By knowing the value of the bulk resistance, the conductivity has been evaluated. The ionic conductivity of CPE is calculated from $\sigma = l/R_b r 2\pi$, where l and r represent the thickness and the radius of the pellet, respectively. R_b is the bulk resistance of the CPE obtained from complex impedance measurements. Variations in ionic conductivity have been observed for various monomer

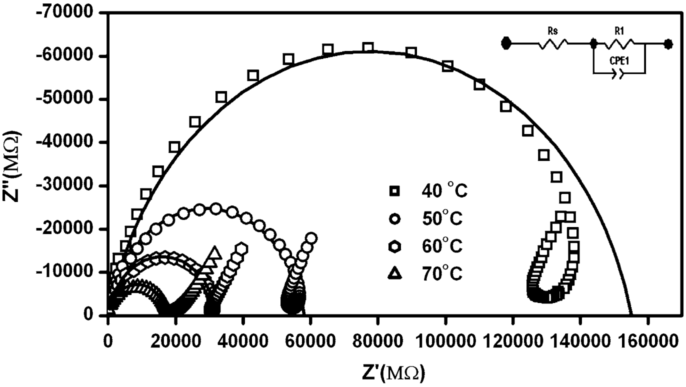

Fig. 9 Impedance spectrum of CPE1 for various temperatures (The *solid line* represents the fitting of the experimental data in accordance with the equivalent circuit)

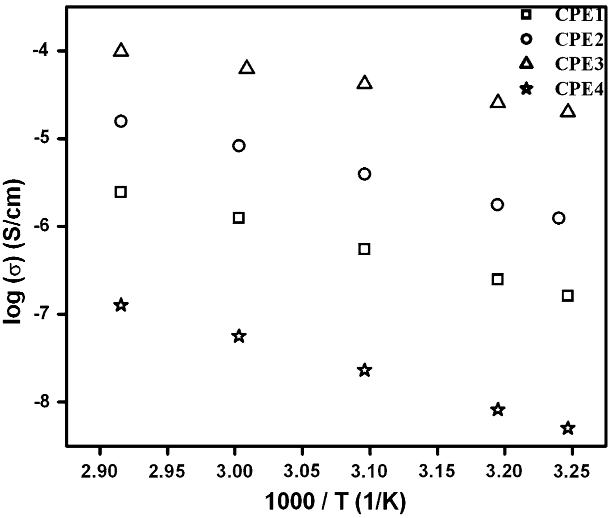

Fig. 10 Ionic conductivity of CPE with various monomer concentrations

concentrations (Table 1). It could be seen from Fig. 10 that the conductivity of CPE1 is 1.4809E−6 S/cm. The maximum ionic conductivity of 4.37804E−5 S/cm is observed for CPE3 (2:1 CuO/Indole w/w ratio) at ambient temperature, and a further increase in the monomer leads to a fall in conductivity. This drop in conductivity may be attributed to an aggregation of CuO nanoparticles that can strongly interact with the polymer chains and immobilize the polymer chains in the process. Although the nature of the filler has an important influence on the conductivity behavior, other factors may also come into play. Moreover, the strong polarizing effect of the bulkier anion can also influence charge transport. This illustrates that ionic conduction in the polymer electrolyte obeys the

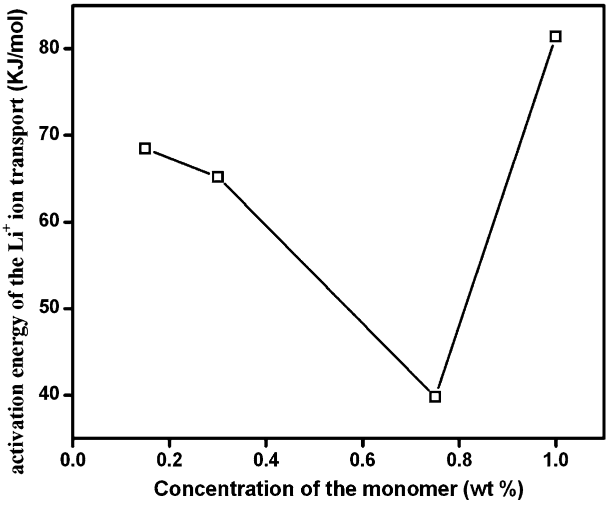

Fig. 11 Activation energy at different monomer concentrations

Vogel–Tamman–Fulcher (VTF) relation, which describes the transport properties in a viscous polymer matrix [16]. It is noted that the increase in temperature leads an to increase in conductivity, as expected since as the temperature increases the polymer expands to produce free volume, which leads to enhanced ionic mobility and polymer segmental motion. The enhancement of ionic conductivity by the CuO nano particles can be explained by the fact that the particles inhibit recrystallization kinetics, helping to retain the amorphous phase down to relatively low temperatures [17]. The activation energy for ion transport can be obtained using VTF model

$$\sigma = \sigma_0 T^{-1/2} \exp\left(-E_a/T - T_0\right)$$

σ is the conductivity, σ_0 is the pre exponential factor, T is the temperature, T_0 is the glass transition temperature, and E_a is the activation energy. Table 1 illustrates the ionic conductivity of CPE and the activation energy for ionic transport. Figure 11 shows that the activation energy for ionic transport decreases after the addition of indole monomer up to 0.75 g, whereas it increases with further addition of indole into the composite. The activation energy falls to 39.80 kJ/mol when the mass fraction of indole equals 0.75 g.

Dielectric properties

Analysis of frequency dependent electrical response of solid electrolytes with disordered structure is a versatile approach for understanding the nature of ionic transport. For this the collected complex impedance data have been analyzed in different formalisms such as permittivity (ε) and electric modulus (M). These complex electrical quantities are interrelated according to the following equation

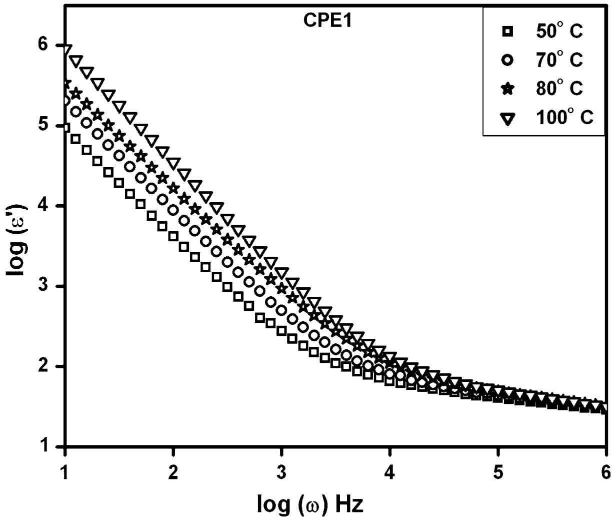

Fig. 12 Plot of log ε' with the frequency of the sample CPE1

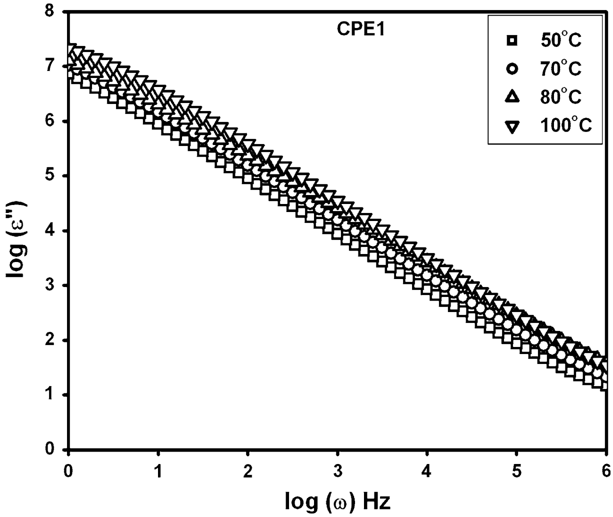

Fig. 13 Plot of log ε'' with the frequency of the sample CPE1

$$M^* = 1/\varepsilon^* = j\omega C_0 Z^*.$$

The value of ε' for CPE decreases with frequency, which is a normal dielectric behavior in polymer nanocomposite. The temperature dependence of the dielectric constant and dielectric loss for all the CPEs are shown in Figs. 12 and 13, respectively. The decrease in ε' takes place when the jumping frequency of the electric charge carriers cannot follow the alternation of ac electric field beyond a certain critical frequency. The analysis of complex permittivity data provides

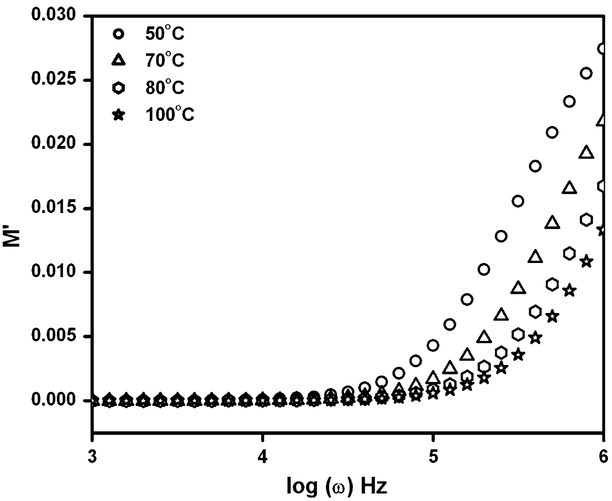

Fig. 14 Frequency dependent electric modulus (M') of the sample CPE1

information about electrode polarization. On the other hand, the analysis of modulus data assumes importance, as the conductivity relaxation becomes prominent due to the suppression of the electrode effects. The high dielectric permittivity values observed at low frequency region can be attributed to the buildup of space charge near the electrode–electrolyte interface which blocks the charge transport. At higher frequencies the permittivity values of the material is found to decrease rapidly and saturate, as the dipoles in the macromolecules hardly will be able to orient in the direction of the applied field. The mobility of charge carriers, and hence their hopping rate, increases with temperature. The dielectric polarization increases causing an increase in dielectric constant and dielectric loss with temperature. Similar trend in the variation of imaginary part of the permittivity (ε'') for CPE with frequency is seen from Fig. 13. The relaxation time decreases with temperature due to high thermal energy supplied to the sample, and hence the dielectric constant increases with temperature. The frequency dependence of M' and M'' at different temperatures for CPE is shown in Figs. 14 and 15. It is seen from the figure that at lower frequencies M' approaches zero indicating negligible contribution of electrode polarization. At higher frequencies, the M' is found to increase gradually with a tendency for saturation. Figure 15 shows the imaginary part of modulus (M'') spectra of sample CPE1 at selected temperatures. The figure clearly shows that the M'' peak shifts towards higher frequency with temperature. The peak frequency is called the relaxation frequency and it increases with temperature because of the thermal activation of the localized electric charge carriers which form the electric dipoles.

The low values of M'', in the low frequency region, indicate negligible contribution of the electrode polarization to the electric modulus. At higher frequencies, M'' spectra show broad and asymmetric peak at a frequency $\omega_{\max}$. This on-Debye behavior can be interpreted as being a consequence of distributions of

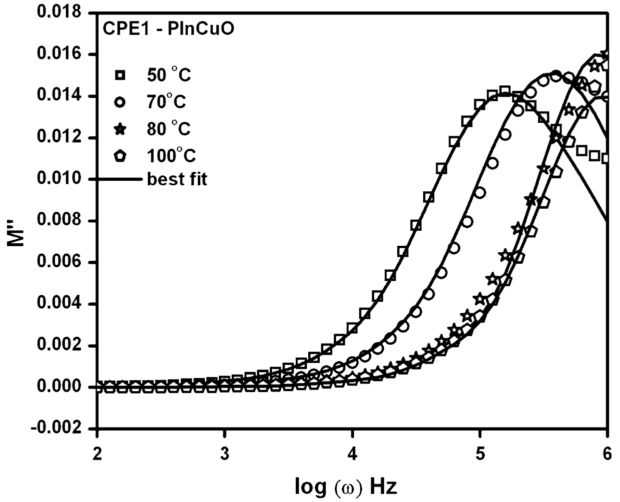

Fig. 15 Frequency dependent electric modulus of the (M'') of the sample CPE1

relaxation time and due to non-exponential approach of electrical functions, defined by the stretched Kohlrausch function [18].

$$\Phi(t) = \exp(-t/\tau)^{\beta}$$

where τ is the characteristics relaxation time and $0 < \beta < 1$ represents the departure of plot from linear exponential ($\beta = 1$). The β parameter determined using the full width at half maxima value of M'' peak is found to be around 0.65 and independent of temperature. The frequency corresponding to $M''_{\max}$ shifts to higher frequencies with increase in temperature. It is observed that the relaxation time decreases with the measuring temperature. The electric dipoles in polymer composites originate from hopping of charge carriers. When the charge carriers are thermally activated, the hopping rate increases and hence the relaxation time decreases with temperature [18].

Conclusion

A $LiClO_4$-based polyindole–CuO CPE was investigated with different ratios of CuO to monomer, the 2:1 CuO/Indole w/w ratio gave a maximum conductivity of 1.95E−5 S/cm at room temperature. The lowering of the crystalline nature of the CPE leads to improved conductivity by the addition of copper oxide nanoparticles. The high conductivity of the CPE is attributed to its high amorphicity, which facilitates the mobility of Li^+ ions. Thus, PInCuO (CPE3) CPE is a potential candidate for lithium ion electrolyte batteries.

Acknowledgment The authors wish to acknowledge the DST-FIST, CSIR, and UGC, Government of India.

References

1. Wang X-L, Mei A, Li M, Lin Y-H, Nana C-W (2007) Polymer composite electrolytes containing ionically active mesoporous SiO_2 particles. J Appl Phys 102:054907–054910
2. Halsey TC, Torr W (1990) Structure of electrorheological fluids. Phys Rev Lett 65:2820–2825
3. Vaia RA, Jandt KD, Kramer EJ, Giannelis DP (1995) Kinetics of polymer melt intercalation. Macromolecules 28:8080–8084
4. Wieczorek W, Such K, Wycislik H, Plocharski J (1989) Modifications of crystalline structure of PEO polymer electrolytes with ceramic additives. J Solid State Ion 36:255–258
5. Fan L, Dang Z, Wei G, Nan C-W, Li M (2003) Effect of nanosized ZnO on the electrical properties of $(PEO)_{16}LiClO_4$ electrolytes. Mater Sci Eng B 99:340–345
6. Liang YP, Ma HZ, Wang B (2004) Synthesis and characterization of a novel polymer electrolyte for lithium- ion battery. Chin Chem Lett 15:234–237
7. Dhanalakshmi K, Saraswathi R (2001) Electrochemical preparation and characterization of conducting copolymers: poly(pyrrole-co-indole). J Mater Sci 36:4107–4115
8. Prakash R, Srivastava RC, Pandey PC (2002) Copper(II) ion sensor based on electropolymerised undoped conducting polymers. J Solid State Electrochem 6:203–208
9. Lagashetty A, Vijayanand H, Basavaraja S, Bedre MD, Venkataraman A (2010) Preparation, characterization, and thermal studies of γ-Fe_2O_3 and CuO dispersed polycarbonate nanocomposites. J Therm Anal Calorim 99:577–581
10. Gandhi S, Hari Hara Subramani R, Ramakrishnan T, Sivabalan A, Dhanalakshmi V, Gopinathan Nair MR, Anbarasan R (2010) Ultrasound assisted one pot synthesis of nano-sized CuO and its nanocomposite with poly(vinyl alcohol). J Mater Sci 45:1688–1694
11. Bhide A, Hariharan K (2006) A new polymer electrolyte system $(PEO)_n$:$NaPO_3$. J Power Sour 159:1450–1457
12. Anantha PS, Hariharan K (2005) Physical and ionic transport studies on poly(ethylene oxide)–$NaNO_3$ polymer electrolyte system. Solid State Ion 176:155–162
13. Bhide A, Hariharan K (2007) Ionic transport studies on $(PEO)_6$:$NaPO_3$ polymer electrolyte plasticized with PEG_{400}. Eur Polym J 43:4253–4270
14. Aravindan V, Vickraman P, Shankarasubramanian N (2007) A study on the blending effect of polyvinyledene fluoride in the ionic transport mechanism of plasticized polyvinyl chloride + lithium perchlorate gel polymer electrolytes. Ionics 13:355–360
15. Ramesh S, Yi LJ (2009) Structural, thermal, and conductivity studies of high molecular weight poly(vinylchloride)-lithium triflate polymer electrolyte plasticized by dibutyl phthalate. Ionics 15:725–730
16. Guo Z, Liang X, Pereira T, Scaffaro R, Hahn HT (2007) CuO nanoparticle filled vinyl-ester resin nanocomposites: fabrication, characterization and property analysis. Compos Sci Technol 67: 2036–2044
17. Wang H, Huang H, Wunder SL (2000) Novel microporous poly(vinylidene fluoride) blend electrolytes for lithium-ion batteries. J Electrochem Soc 147:2853–2861
18. Rhoo HJ, Kim HT, Park JM, Hwang TS (1997) Ionic conduction in plasticized PVC/PMMA blend polymer electrolytes. Electrochim Acta 42:1571–1579